

XPS and SIMS study of aluminium native oxide modifications induced by Q-switched Nd:YAG laser treatment

V. Barnier,^{1*} O. Heintz,¹ D. E. Roberts,² R. Oltra¹ and S. Costil³

¹ Laboratoire de Recherches sur la Réactivité des Solides, UMR 5613 CNRS Université de Bourgogne, 21078 Dijon Cedex, France

² National Laser Centre, Lynwoodridge, Pretoria 0001, South Africa

³ Laboratoire LERMPS, Université de technologie de Belfort et Montbéliard, 90010 Belfort Cedex, France

Received 1 July 2005; Revised 7 November 2005; Accepted 7 November 2005

During laser cleaning of aluminium in ambient atmosphere, modifications of the metal surface can be induced by transient thermal effects. This work aims to characterize the modification of the aluminium oxide layer on pure aluminium for a wide range of power per area using a Q-switched Nd:YAG (1064 nm) laser with two pulse durations, 10 and 180 ns. Experiments were carried out with single laser shots in ambient air at fluences (e.g. energy per area) below the ablation regime.

For 10-ns pulses with fluences between 0.7 and 1.7 J/cm², X-ray photoelectron spectroscopy (XPS) and secondary ion mass spectroscopy (SIMS) revealed thermal oxidation with an increase of the oxide-layer thickness for 0.7–1.3 J/cm². Above a threshold at about 1.3 J/cm² the oxide thickness decreased. The Mixing Roughness Model was used for the SIMS depth profile.

For 180-ns pulses with fluences between 2.1 and 4.3 J/cm², and therefore much lower power per area than with the 10 ns pulses, XPS showed a variation of surface composition with a different behaviour for 2.1–2.9 J/cm² compared to 3.1–4.3 J/cm². However, no significant changes of the average thickness of the oxide layer were found. Copyright © 2006 John Wiley & Sons, Ltd.

KEYWORDS: laser cleaning; aluminium; surface modification; XPS; SIMS; MRI model

INTRODUCTION

In recent years, short-pulse lasers have been shown to be suitable tools for cleaning applications due to their ability to deliver high power per unit area to only the surface region of a workpiece.¹ Generally, oxides, carbon and oils have to be removed from a metallic surface before its final use. In the ideal case, the laser energy necessary to remove contaminants should be below a threshold value to prevent substrate modifications and damage. Conversion of absorbed energy via collisional processes into heat is one of the important effects that occur during the laser interaction. For reactive metallic substrates treated under ambient atmosphere, a limited oxidation is sometimes considered to explain the modifications of surface properties (adhesion, corrosion resistance). These phenomena have been investigated in detail for silicon,² but relatively little work has been reported for aluminium,³ especially for the fluence range considered in this work (thermoelastic range of interaction for metallic surfaces).

The objective of this work was to investigate the modification of a pure aluminium surface by XPS and SIMS analysis, particularly the native oxide evolution, after irradiation over

a wide range of power per unit area by a Nd:YAG laser with two different pulse lengths.

EXPERIMENTAL

The samples were 1.3-mm-diameter and 1-mm-thick discs of 99.99% aluminium (Goodfellow). They were mechanically polished using grit papers of grade 1200–4000, 3–1 µm diamond suspensions and finally a colloidal suspension of 0.05 µm SiO₂. A sample with a 1-µm Al₂O₃ coating with physical vapour deposition (PVD) was used to calibrate the sputtering rate during SIMS analysis.

Two Q-switched Nd:YAG lasers with fibre optic beam delivery with a wavelength of 1064 nm and pulse durations of 180 ns (US Laser) and 10 ns (Quantel) were used. The first one gave a 0.8-mm diameter beam with a 'top hat' energy distribution. The second one gave two rectangular and homogeneous spots, which allowed a 1-cm² area to be treated.

The XPS analyses were realized with two instruments. For the 1-cm² treated samples, measurements were performed using a SIA 100 Riber system. A Mg K α X-ray source with a power of 240 W and a spectrometer, MAC 2 Riber, with an energy resolution (width of Ag 3d^{5/2}) of 2 eV for spectra and of 1.27 eV for window were used. For samples treated with the 0.8-mm diameter beam, analyses were carried out on a Physical Electronics Quantum 2000 instrument using a

*Correspondence to: V. Barnier, Laboratoire de Recherches sur la Réactivité des Solides, UMR 5613 CNRS Université de Bourgogne, 21078 Dijon Cedex, France. E-mail: vincent.barnier@u-bourgogne.fr
Contract/grant sponsor: Councils of Bourgogne.
Contract/grant sponsor: Territoire de Belfort.

100- μm , focused, monochromated Al $K\alpha$ beam with a power of 17.86 W. The energy resolution was 1 eV for wide scans and 0.25 eV for narrow scans. All the data were analysed using the software Casa XPS.

The SIMS experiments were performed using a MIQ 256 Riber instrument with primary Ar^+ ions with an energy of 4 keV and a sample current of 5 nA. The incidence angle was 45° and the scanning area was $280 \times 400 \mu\text{m}^2$.

The residual pressure of the analysis chambers for the XPS and SIMS measurements was maintained below 10^{-9} mbar.

RESULTS AND DISCUSSION

In order to study changes of the native oxide for laser interaction over a wide range of power per unit area, two sets of experiments were realized: one with a laser pulse duration of 10 ns and fluences between 0.7 and 1.7 J/cm^2 (70–170 MW/cm²), and a second one with a laser pulse duration of 180 ns and fluences between 2.1 and 4.3 J/cm^2 (11.6–24 MW/cm²). Each laser exposure was made with a single shot in ambient atmosphere.

Laser treatment with 10-ns pulses

XPS studies of the effects induced by laser treatment were estimated from the O 1s, Al 2p and C 1s photoelectron peaks. Since significant changes were mainly observed on Al 2p, data analyses were focused on this peak. Oxidized (Al^{3+}) and metallic (Al^0) Al 2p peaks were fitted according to procedure described in Ref. 4, after subtraction of an inelastic background (Tougaard) over the binding energy range of 70 to 80 eV.⁵

For untreated and laser-treated samples, no significant change of the oxidized peak position was observed, but a variation of the ratio between I_o and I_m , the intensities of Al^{3+} and Al^0 components, clearly appeared. Therefore, calculation of oxide thicknesses was performed using Eqn (1). C_m and C_o , the theoretical molar densities of Al in metal and in oxide were 100.14 and 71.85 mol/dm^3 , respectively.⁶ The inelastic mean free paths of photoelectrons propagating through the metal λ_m and oxide λ_o , were taken as 2.23 and 2.4 nm.⁷ The angle of photoelectron detection θ with respect to specimen surface was 90°.

$$d = \lambda_o \sin \theta \ln \left(\frac{C_m \lambda_m}{C_o \lambda_o} \cdot \frac{I_o}{I_m} + 1 \right) \quad (1)$$

Figure 1 shows the evolution of the oxide thickness d with the fluence applied, and exhibits an increase for fluences from 0.7 to 1.3 J/cm^2 . This variation can be explained by the increase in maximum temperature reached during the transient laser heating of the surface when the fluence increases. Above 1.3 J/cm^2 , the thickness decreases dramatically presumably due to coexistence of oxide-layer growth and ablation.

SIMS depth profiles on samples treated with 0.7, 1 and 1.3 J/cm^2 were performed in order to confirm the variation of oxide-film thickness with fluence. On first approximation, the position of the interface between the oxide and metal can be correlated with the intersection between AlO^+ and Al_3^+ signals. This position can be

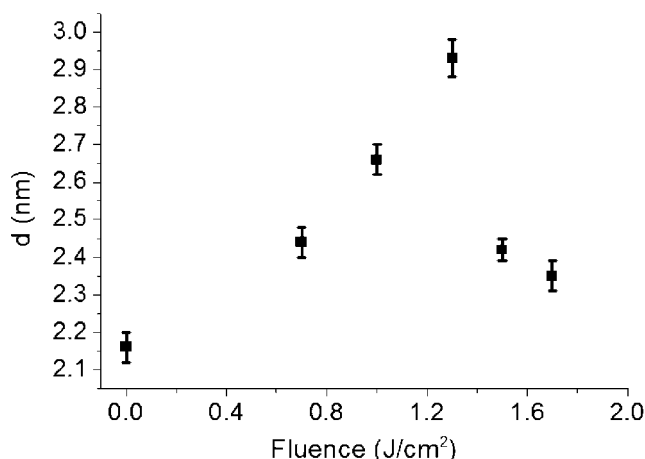


Figure 1. Oxide thickness (d) estimated with XPS versus fluence for 10 ns pulses.

determined more accurately by fitting the Al_3^+ signal with the mixing-roughness-information (MRI) depth model⁸ described by Eqns (2), (3) and (4), where z is the depth and I_o the intensity of 100% homogeneous bulk. The interface position z_1 was calculated simultaneously with the atomic mixing length w and the roughness σ , which alter the shape of the depth profile. A -3σ and $+3\sigma$ windowing function was used for convolution computations.

$$I|\text{Al}_3^+(z) = g1(z) \otimes g2(z) \quad (2)$$

$$g1(z) = I_o \times [1 - \exp(-(z - z_1 + w)/w)] \quad \text{for } z \geq z_1 - w \quad (3)$$

$$g2(z) = \frac{1}{\sqrt{2\pi}\sigma} \cdot \exp(-z^2/2\sigma^2) \quad (4)$$

The time/depth scale was calibrated with measurements of sputter rate on pure aluminium and PVD-coated Al_2O_3 sample. Experimental and theoretical curves of SIMS depth profiles analysis are illustrated in Fig. 2.

The increases of the values of the intersection point of AlO^+ and Al_3^+ curves and the interface position z_1

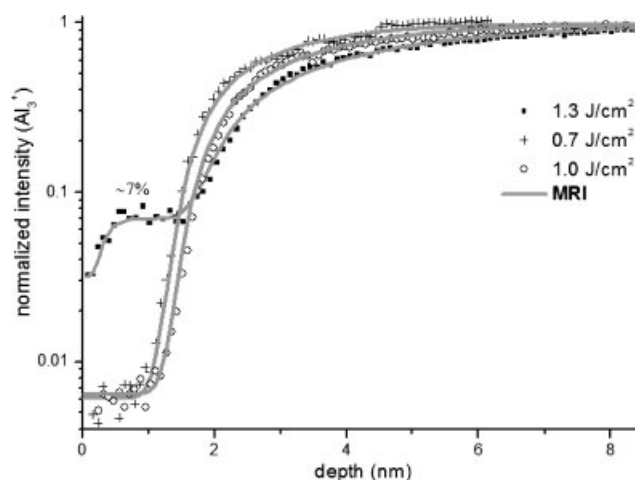


Figure 2. Al_3^+ SIMS depth profiles for aluminium samples irradiated with 10-ns pulses at 0.7, 1.0 and 1.3 J/cm^2 . The grey curves represent optimum fits using the MRI model.

(determined with MRI fit) with the laser fluence used (Table 1) were in good agreement with the increase of oxide thickness observed with the XPS. As expected, it can be noted that the mixing length increases with the thickness of the oxide layer. The intensity profile of Al_3^+ for the sample treated with 1.3 J/cm^2 exhibits two interfaces. The ratio of the intensity between the first and the second step suggests the presence of holes in the oxide with approximately 7% coverage, but it is not possible to say anything about their distribution.

For this range of power per unit area ($70\text{--}170 \text{ MW/cm}^2$), XPS and SIMS show that the transient laser heating of the surface induces a gradual increase of the oxide thickness due to thermal oxidation for fluences from 0.7 to 1.3 J/cm^2 . The smaller thicknesses calculated for samples irradiated with 1.5 and 1.7 J/cm^2 , as well as the two interfaces observed with SIMS profile for the sample treated at 1.3 J/cm^2 , indicate probably a threshold above which the native oxide is removed.²

Laser treatment with 180-ns pulses

For the second set of experiments, all laser impacts were made on the same pure aluminium sample with six different fluences (Table 2). XPS studies were also carried out using the Al 2p, O 1s and C 1s photoelectron peaks. The components for Al 2p peak were found using the procedure detailed in Ref. 4. Shirley background was removed from C 1s and O 1s peaks over the binding energy ranges of $280\text{--}295$ and $525\text{--}540 \text{ eV}$, and Voigt convolution of Gaussian and 30% of Lorentzian were used for all components.

No variation of the intensity ratio between aluminium oxide and metallic Al 2p peaks was observed. This indicates that the average thickness of the film does not change with the fluence. It was also noted that without correction of the charge effect, the metallic Al 2p peak appeared always at the same binding energy (73 eV).

Decomposition of O 1s gave a proportion of OH^- component more important for 2.1 , 2.4 and 2.9 J/cm^2 than for the untreated area, while for 3.1 , 3.8 and 4.3 J/cm^2 the symmetric form and width of O 1s indicates the presence of only one component (O^{2-}) (Table 2). These analyses show an evolution of the oxide composition with the fluence used for laser treatment, and in particular two different behaviours for low (2.1 , 2.4 and 2.9 J/cm^2) and high (3.1 , 3.8 and 4.3 J/cm^2) fluences.

C 1s envelopes, after charge correction, were fitted with components C–C (284.5 eV), CO_2^- ($288.9 \pm 0.05 \text{ eV}$), C– CO_2^- ($285.3 \pm 0.05 \text{ eV}$) and C–OX ($286.8 \pm 0.07 \text{ eV}$ with $X = \text{H}, \text{CH}_y$)⁴ (Table 2). The most important proportions of CO_2^- and C– CO_2^- components in C 1s peak are found for the low fluences (2.1 , 2.4 and 2.9 J/cm^2). On the other hand, for high fluences (3.1 , 3.8 and 4.3 J/cm^2), in order to take account of the asymmetric form at the lower binding energy and the width of the C 1s peak, two peaks (283.8 eV , 283 eV) were introduced that could correspond to C–Al–O and C–Al bonding (Table 2). Because transient heating is more important at these higher fluences, diffusion of carbon contaminants into the substrate could occur during laser impact.

If no attempts were made to calibrate the C 1s peak position, considering that the position of Al 2p metallic

Table 1. Depth of aluminium oxide/aluminium interface, mixing and roughness parameters corresponding to MRI calculations for fit curves illustrated in Fig. 2. The table also shows the intersection point of the AlO^+ and Al_3^+ secondary ions signals

Fluence (J/cm^2)	z_1 – Interface position (nm)	w – Mixing length (nm)	σ – Roughness (nm)	$\text{AlO}^+ - \text{Al}_3^+$ intersection (nm)
0.7	2.88 ± 0.03	1.38 ± 0.04	0.22 ± 0.03	1.80 ± 0.05
1.0	3.41 ± 0.07	1.84 ± 0.03	0.21 ± 0.02	2.17 ± 0.05
1.3 (1st step)	0.39 ± 0.02	0.15 ± 0.05	0.10 ± 0.01	–
1.3 (2nd step)	3.87 ± 0.02	2.09 ± 0.03	0.20 ± 0.01	2.61 ± 0.05

Table 2. Al $2p_{3/2}$ metallic–Al 2p oxide energy separation and proportions of the different components used to fit C 1s and O 1s for 180-ns pulses, derived from XPS measurements

Fluence (J/cm^2)	Distance Al $2p_{3/2}$ – Al^{3+} (eV)	O 1s		C 1s					
		O^{2-} (%)	OH^- (%)	C–C (%)	C– CO_2^- (%)	CO_2^- (%)	C–OX (%)	C–Al–O (%)	C–Al (%)
0	2.95	80.9	19.1	87.8	3.6	7.1	1.5	0	0
4.3	2.45	100	0	55.1	3.1	3.4	0	16.6	21.8
3.8	2.5	100	0	54.6	6.9	3.9	0	22	12.6
3.1	2.55	100	0	52.7	4.6	2	0	33	8.7
2.9	3.25	72.6	27.4	78.3	4.1	16.4	1.2	0	0
2.4	3.3	66.5	33.5	73.4	6.6	16.6	3.4	0	0
2.1	3.3	72.1	27.9	82.2	4.6	12.5	0.7	0	0

peak does not change, a shift of the Al 2p oxide peak is observed. Comparing with the untreated area, a shift of the Al 2p oxide peak toward the upper binding energy for 2.1, 2.4 and 2.9 J/cm² and lower binding energy for 3.1, 3.8 and 4.3 J/cm² are observed. The distance between Al 2p_{3/2} metallic and Al 2p oxide peaks calculated after curve fitting (Table 2) shows a decrease when the laser fluence used increases, which can be due to differences of composition as we previously saw with O 1s and C 1s peaks. Actually, a shift toward upper and lower binding energies for low and high fluences is also noted for O 1s and C 1s because of charging effects. If a calibration is made for all peaks with C 1s at 284.5 eV, the position of Al 2p oxide peak (74.1 ± 0.03 eV) for low fluences is still different from the Al 2p oxide peak of the untreated area (74.3 eV), while for high fluences this value is closer (74.38 ± 0.05 eV). Explanations for the differences of charging effects can be a morphological change, defects or oxygen vacancies induced by laser on the oxide layer.⁹ The Al 2p metal peak probably does not shift because the work function for Al metal is not very sensitive to these changes. Consequently the shift of the Al 2p oxide peak for high fluences is mainly due to charging effects, while for the low fluences, both composition and charging effects must be taken into account.

CONCLUSIONS

Modifications of the native oxide took place during irradiation of pure aluminium in air by single pulses of Q-switched Nd:YAG laser. These modifications depend on the range of power per unit area used for treatment.

For 70 to 170 MW/cm², using a 10-ns pulse, transient heating of the surface induces a thickness change of the aluminium oxide layer. In the range 0.7–1.3 J/cm², growth of the oxide was observed. Above 1.3 J/cm², a threshold is observed owing to the coexistence of oxide removal and thermal oxidation.

For 11.6 to 24 MW/cm², using a 180-ns pulse, no variation of the average thickness of the oxide layer was seen. But composition and differences of charging effects were observed with XPS on the basis of a shift of the Al 2p oxide peak. Two types of behaviour were identified. In the range of 2.1–2.9 J/cm², the amount of hydroxide, carboxylic and carboxylate species seems to be more important, while for 3.1–4.3 J/cm² no hydroxide species were detected but a diffusion of carbon contaminants was indicated.

Changes of aluminium surface properties due to variations of composition, structure and thickness of the oxide layer during laser cleaning are very important for many industrial applications, particularly adhesion. It seems that removing carbon from the surface can be problematic. Work is in progress to define the best condition to reach this goal.

Acknowledgements

Vincent Barnier would like to thank the regional councils of Bourgogne and Territoire de Belfort for financial support.

REFERENCES

1. Boquillon JP, Bresson P, Berger H. *Procédé de nettoyage de surface par laser impulsif* (Patents France no 8900496, USA no 5 151 134, European no 904001 229), 1992.
2. Cohen C, Siejka J, Pribat D, Berti M, Drigo AV, Bentini GG, Jannitti E. *Journal De Physique* 1983; **44**: 179.
3. Dimogerontakis T, Oltra R, Heintz O. *Appl. Phys. A* 2004; **00**: 1, DOI: 10.1007/s00339-004-31-7.
4. Alexander MR, Beamson G, Bailey P, Noakes TCQ, Skeldon P, Thompson GE. *Surf. Interface Anal.* 2003; **35**: 649.
5. Tougaard S. *Surf. Interface Anal.* 1988; **11**: 453.
6. Seah MP. In *Practical Surface Analysis* (2nd edn), vol. 1, Briggs D, Seah MP (eds). John Wiley: Chichester, UK, 1990; 201.
7. Tanuma S, Powell CJ, Penn DR. *Surf. Interface Anal.* 1991; **17**: 911.
8. Hofman S. *Surf. Interface Anal.* 1994; **21**: 673.
9. Baer DR, Windisch CF, Engelhard MH, Zavadil KR. *J. Surf. Anal.* 2002; **9**(3): 396.